American Journal of Pathology, Vol. 164, No. 1, January 2004

Animal Model

Rapid Neurofibrillary Tangle Formation after Localized Gene Transfer of Mutated Tau

Ronald L. Klein,* Wen-Lang Lin,† Dennis W. Dickson,† Jada Lewis,‡ Michael Hutton,‡ Karen Duff,§ Edwin M. Meyer,¶ and Michael A. King‖**

From the Department of Pharmacology and Therapeutics, Louisiana State University Health Sciences Center, Shreveport, Louisiana; the Departments of Pathology† and Neuroscience,‡ Mayo Clinic, Jacksonville, Florida; the Departments of Pharmacology and Therapeutics¶ and Neuroscience,‖ University of Florida College of Medicine and McKnight Brain Institute, Gainesville, Florida; the Malcom Randall Veteran's Administration Medical Center,** Gainesville, Florida; and the Center for Dementia Research,§ Nathan Kline Institute, Orangeburg, New York*

Neurofibrillary pathology was produced in the brains of adult rats after localized gene transfer of human tau carrying the P301L mutation, which is associated with frontotemporal dementia with parkinsonism. Within 1 month of *in situ* transfection of the basal forebrain region of normal rats, tau-immunoreactive and argyrophilic neuronal lesions formed. The fibrillar lesions had features of neurofibrillary tangles and tau immunoreactivity at light and electron microscopic levels. In addition to neurofibrillary tangles, other tau pathology, including pretangles and neuropil threads, was abundant and widespread. Tau gene transfer to the hippocampal region of amyloid-depositing transgenic mice produced pretangles and threads, as well as intensely tau-immunoreactive neurites in amyloid plaques. The ability to produce neurofibrillary pathology in adult rodents makes this a useful method to study tau-related neurodegeneration. ***(Am J Pathol 2004, 164:347–353)***

Tauopathies are a group of progressive neurodegenerative diseases characterized by abnormal accumulations of the microtubule-associated protein tau.[1,2] In the adult nervous system tau is preferentially localized to axons,[3] where it contributes to dynamic properties of microtubules, including fast axonal transport of vesicular structures.[4] In human tauopathies tau is phosphorylated excessively and on amino acid residues not usually modified,[5–7] resulting in abnormal conformations[8,9] that are likely to interfere with a variety of intracellular functions.[10] The selective axonal compartmentation of tau is also lost.[11] Intracellular lesions develop as nonfibrillar aggregates referred to as "pretangles." Throughout time these progress into argyrophilic, filamentous, neurofibrillary tangles (NFTs). At the electron microscopic level, pathological tau filaments take a variety of forms, including paired helical filaments and straight filaments, which are relatively disease-specific and related to the tau isoform composition of fibrils.[6,7] In Alzheimer's disease (AD), NFTs composed of 3R and 4R tau (isoforms containing three or four repeats of a 31- to 32-residue motif in the microtubule-binding domain) usually appear as paired helical filaments. In the most common tauopathies, which are associated with preferential accumulation of 4R tau, the filaments are straight or twisted ribbons.

NFTs characterize the neurodegeneration found in the tauopathies, but they are also a diagnostic necessity for AD. NFTs have been difficult to study experimentally because they rarely develop in subprimates. As a result it is not fully understood how pretangles and NFTs are linked to neurodegeneration or to amyloid plaques, the other major histopathological lesion in AD. Discovery of disease-related mutations in the tau gene has led to animal models of NFTs. The P301L mutation, which is the most common cause of frontotemporal dementia with parkinsonism linked to chromosome 17 (FTDP-17; 1), has been used in developing mouse models that share structural and biochemical features with human tauopathies.[12–14]

Somatic cell gene transfer can complement the whole animal transgenic approach for analyzing the function of gene products. The onset of expression can be controlled and the expression targeted to specific brain regions. Inducing expression in an adult could produce disease more rapidly than in transgenic lines that may

Supported by National Institute on Aging (grant AG10485).

Accepted for publication September 26, 2003.

Address reprint requests to Ronald L. Klein, Ph.D., Department of Pharmacology and Therapeutics, LSUHSC, 1501 Kings Hwy., Shreveport, LA 71130. E-mail: klein@lsuhsc.edu.

experience adaptation during development. Viral vector-based systems have led to nigrostriatal degeneration models in rats via α-synuclein gene transfer.[15] We used the adeno-associated virus (AAV) system to rapidly generate neurofibrillary pathology in rats. Another advantage of somatic cell gene transfer is combining transgenes, which we studied by applying the vector to a transgenic line, amyloid-bearing mice that express mutant amyloid precursor protein and presenilin 1.[16]

Materials and Methods

DNAs, Transfections, Western Blots

DNAs to be expressed were incorporated into expression cassettes that are flanked by the AAV serotype 2 terminal repeats, the only remaining sequence (and 4%) of the AAV-2 genome. The hybrid cytomegalovirus/chicken β-actin (CBA) promoter[17] was used for all constructs and in some cases, the 3′ enhancer woodchuck hepatitis virus posttranscriptional regulatory element (WPRE).[18] Control green fluorescent protein (GFP) plasmids were described previously.[19] Constructs were made for the P301L form of tau including exons 2/3 (4R2N) 30.[14] Western blots were performed with 293 cells transfected with the tau DNAs, primary neuronal cultures treated with tau AAVs, and brain tissue injected with the tau AAVs, using a human tau-specific antibody (T-14; Zymed, South San Francisco, CA) and an antibody against hyperphosphorylated tau (CP13; P. Davies, Albert Einstein College of Medicine, Bronx, NY). The primary neuron preparations were from whole brains of newborn Sprague-Dawley rats as previously described.[19,20] Ten days after plating, the AAV was added and cells were harvested 5 days later for tau immunoblots. Samples of brain tissue injected with tau AAV vectors were also run for tau immunoblots by dissecting the medial septum/vertical limb of diagonal band, and preparing the tissue for Western blot. All samples were normalized for protein content by Bradford assay and subjected to 12% sodium dodecyl sulfate-polyacrylamide gel electrophoresis.

Vector Packaging and Titering

Packaging of plasmids in recombinant AAV serotype 2 was based on published methods.[21] Human embryonic kidney 293 cells were transfected with an AAV terminal repeat-containing plasmid in an equimolar ratio with the AAV helper plasmid pDG.[22] The cell sample is applied to a discontinuous gradient of iodixinol (OptiPrep; Nycomed) and centrifuged. The AAV was then removed and added to a heparin (Sigma Chemical Co., St. Louis, MO) affinity column and the eluent was concentrated and washed using Millipore Biomax 100 Ultrafree-15 U (Millipore, Bedford, MA). AAV vector stocks were titered for physical particles or copies of vector genomes by dot-blotting against standard curves of known amounts of DNA using the nonradioactive Psoralen-Biotin and BrightStar kits from Ambion (Austin, TX). Titers for the AAVs that were used were between 1×10^{12} and 1×10^{13} particles per ml.

Study Participants and Stereotaxic Injections

Male Sprague-Dawley rats (3 months old) were anesthetized with a cocktail of 3 ml of xylazine (20 mg/ml), 3 ml of ketamine (100 mg/ml), and 1 ml of acepromazine (10 mg/ml) administered intramuscularly at a dose of 0.5 to 0.7 ml/kg. The injection coordinates for the medial septum were 0.7 mm bregma, 0.2 mm lateral, 7.0 mm ventral.[23] Virus stocks were injected through a 27-gauge cannula connected via 26-gauge inner diameter polyethylene tubing to a 10-μl Hamilton syringe mounted to a CMA/100 microinjection pump. The pump delivered 3 μl at a rate of 0.2 μl/min, and the needle remained in place at the injection site for 1 additional minute. The cannula was removed slowly (throughout 2 minutes), and the skin was sutured and the animal was placed on a heating pad until it began to recover from the surgery, before being returned to their individual cages. Two-month-old double-transgenic PS1/APP mice[16] were injected with AAV vectors in the hippocampus, −2.1 mm bregma, 1.2 mm lateral, 2.0 mm ventral.[24] The anesthetic for mice was isoflurane using a gas anesthesia system. The dose for induction was 3 to 4% isoflurane in oxygen and 1 to 2% for maintenance. Two μl of AAV vector was injected with a 30-gauge needle. All animal care and procedures were in accordance with institutional IACUC and NIH guidelines.

Histological Staining for Light and Electron Microscopy

Anesthetized animals were perfused with cold phosphate-buffered saline (PBS), followed by cold 4% paraformaldehyde in PBS. The brain was removed and immersed in fixative overnight at 4°C. For standard immunohistochemistry, the brain was equilibrated in a cryoprotectant solution of 30% sucrose/PBS at 4°C. Coronal sections (50 μm thick) were cut on a sliding microtome with freezing stage. Antigen detection was conducted on free-floating sections by incubation in a blocking solution (2% goat serum/0.3% Triton X-100/PBS) for 1 hour at room temperature, followed by primary antibody incubation overnight at 4°C on a shaking platform. Before blocking, endogenous peroxidase was quenched by incubation in 0.1% H_2O_2/PBS for 10 minutes. The sections were washed in PBS, and incubated with biotinylated goat anti-rabbit or goat anti-mouse secondary antibody (1:1000; DAKO, Carpinteria, CA) for 1 hour at room temperature. The sections were washed with PBS and labeled with horseradish peroxidase-conjugated Extravidin (1:1000, Sigma) for 30 minutes at room temperature. Development of tissue labeled with horseradish peroxidase was conducted with a solution of 0.67 mg of diaminobenzidine (Sigma), 0.13 μl of 30% H_2O_2 per ml of 80-mmol/L sodium acetate buffer containing 8 mmol/L imidazole and 2% $NiSO_4$. Peroxidase-stained sections were mounted on Fisher Superfrost Plus glass slides

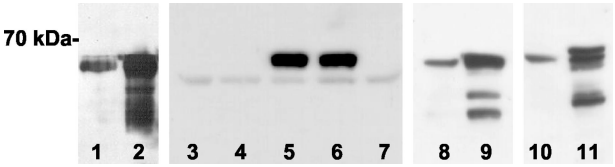

Figure 1. Tau AAV vector expression *in vitro* and *in vivo*. The form of tau was the human P301L including exons 2, 3, 10 (4R2N), and the main protein band produced ran at ~70 kd, as expected. **Lanes 1** and **2**: Tau T-14 immunoblot, 20 μg of either the pCB-Tau (**lane 1**) or the pTau-W (**lane 2**) DNAs were transfected into HEK 293 cells, 20 μg of protein per lane. **Lanes 3** to **7**: Tau T-14 immunoblot, 4×10^{10} particles of either the pCB-Tau AAV (**lanes 3** and **4**) or the pTau-W AAV (**lanes 5** and **6**) was added to day 10 neonatal rat whole brain neuronal cultures. After 5 days, the 70-kd band was detected only in cultures that were treated with the WPRE-containing vector. **Lane 7**: Untreated primary neuron culture sample, all samples had a similar band ~60 kd, 20 μg of protein in **lanes 3** to **7**. **Lanes 8** and **9**: Tau T-14 immunoblot, dissected and homogenized basal forebrain after injection of 1×10^{10} particles of the pCB-Tau AAV (**lane 8**, 6 months after injection) or 1×10^{10} particles of the pTau-W AAV (**lane 9**, 1 month after injection), 70 μg of protein per lane. **Lanes 10** and **11**: Hyperphosphorylated tau antibody CP13 immunoblot, pCB-Tau and pTau-W as in **lanes 8** and **9**.

(Fisher Scientific, Pittsburgh, PA), dehydrated in a series of ethanol and xylene incubations, and coverslipped with Eukitt (Electron Microscopy Sciences, Fort Washington, PA). Primary antibodies for immunostaining included: GFP (1:2000; Molecular Probes, Eugene, OR); Tau T-14 (1:2000, Zymed); anti-NFT (1:200; Chemicon, Temecula, CA); CP13 (1:200; P. Davies, Albert Einstein College of Medicine, Bronx, NY); Alz-50 (1:200, P. Davies); MC-1 (1:500, P. Davies); Ab-39 (1:500; S. H. Yen, Mayo Clinic Jacksonville, Jacksonville, FL); E-1 (1:500, S. H. Yen); AT100 (1:500; Endogen); 6E10 (1:1000; Serotec, Oxford, UK). Some of the markers were visualized with immunofluorescence using tetramethyl rhodamine-conjugated or aminomethylcoumarin-conjugated secondary antibodies (1:500; Jackson ImmunoResearch, West Grove, PA). Fluorescent samples were coverslipped with glycerol-gelatin (Sigma). For Gallyas silver staining and immunoelectron microscopy, the animals were perfusion-fixed and the brains were extracted and immersed in fixative overnight as above. The brains were then placed in PBS. Tissue blocks of the medial septum/vertical limb of diagonal band were paraffin-embedded for Gallyas or plastic-embedded for immunoelectron microscopy as described.[12,14] Gallyas samples were counterstained for hematoxylin and eosin. For transmission electron microscopy, animals were perfused with normal saline and then 2.5% glutaraldehyde/2% formaldehyde in 0.1 mol/L of sodium cacodylate buffer. The brains were immersed in fixative overnight and then placed in 0.1 mol/L of sodium cacodylate before processing for plastic embedding.

Results

DNA for P301L mutant tau was incorporated into two AAV-2 expression plasmids.[19] The pTau-W construct contained CBA promoter and the WPRE, and a second construct, pCB-Tau, contained only the CBA promoter. Protein extracts of cells transfected with either vector produced a major band ~70 kd on Western blots for human-specific tau (Figure 1), close to the predicted size of 66 kd for the longest form of tau. The WPRE construct appeared to produce more tau expression under the same experimental conditions (Figure 1, lanes 1 and 2). The P301L tau AAV vectors were evaluated in primary neuron cultures and the rat brain. Tau expression was detected in primary neuronal cultures after 5 days with the pTau-W AAV vector, but no expression was detected from similar treatments with pCB-Tau AAV (Figure 1, lanes 3 to 7). The WPRE therefore boosted tau expression in neuronal cultures as previously reported for GFP.[19] Tau transgene expression was detected on Western blots after injections of the vectors into the medial septal region of the basal forebrain of 3-month-old male Sprague-Dawley rats. Immunoblots for total human tau (T-14; Figure 1, lanes 8 and 9) or hyperphosphorylated tau (CP13; Figure 1, lanes 10 and 11) demonstrated expression *in vivo* for both constructs.

The control GFP AAV led to robust expression in the rat basal forebrain (Figure 2, a and b). Within 3 weeks of injection of tau vectors, many neurons around the injection path contained human tau identified by immunofluo-

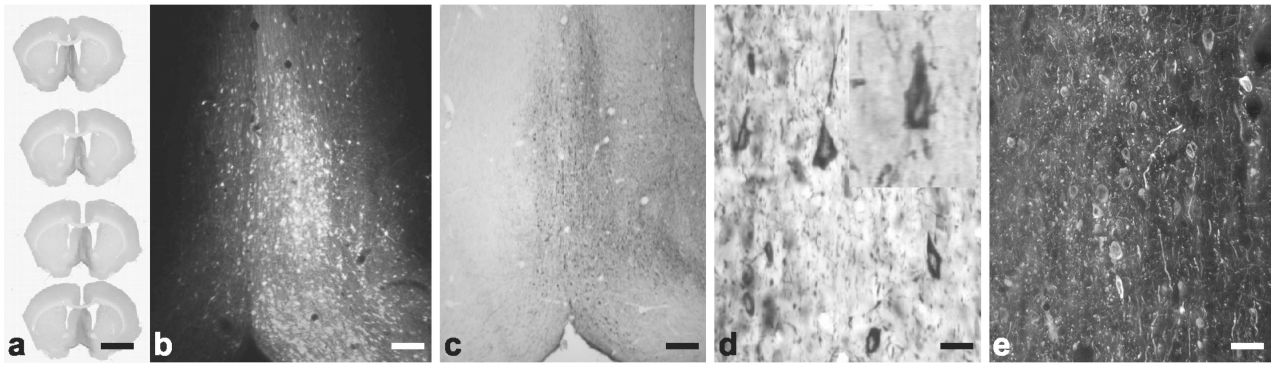

Figure 2. GFP and tau expression in the rat basal forebrain. **a:** The medial septal nucleus/diagonal band was injected, leading to widespread expression of GFP immunoreactivity throughout this area. Serial sections from one brain injected with the control pGFP AAV[19], 1×10^{10} particles in 3 μl, 2 months after injection. **b:** Native GFP fluorescence after the unilateral injections as in **a**, which is not as sensitive in detecting GFP expression as the immunostaining in **a**. **c:** Human-specific Tau T-14 staining 3 weeks after injecting the pCB-Tau AAV (1×10^{10} particles in 3 μl) showing widespread expression of the human tau in the same area as **a** and **b**. **d:** The cells expressing T-14 immunoreactivity had sharp-pointed edges, not unlike in appearance to flame-shaped NFTs. **Inset**, higher magnification. **e:** CP13-hyperphosphorylated tau immunoreactivity, 2 months after injection of pTau-W AAV (1×10^{10} particles; immunofluorescence). The expression pattern for CP13 was similar to that of total tau T-14 immunoreactivity at all intervals tested and with both tau vectors. Scale bars: 4 mm (**a**); 150 μm (**b**); 200 μm (**c**); 25 μm (**d**); 50 μm (**e**).

rescent or immunoperoxidase labeling. Neurons, but not glia, were immunoreactive and labeling was present in perikarya, dendrites, and neuritic arbors. The expression was localized to the medial septum (1 to 1.5 mm anterior and posterior from the injection site) ipsilateral to the injection (Figure 2c). Tau-immunoreactive axons were detected throughout the ipsilateral fimbria, fornix, and hippocampus. The human-specific tau antibody T-14 did not label any structures in rat brain tissue after sham injections or transduction with control vector. Tau expression persisted for at least 8 months after injections, the longest interval tested in rats. Tau immunoreactivity was dense in neuronal perikarya, and the cells had distorted cytological features that differed from normal pyramidal neurons (Figure 2d), resembling flame-shaped NFTs. Immunolabeling for several antibodies against hyperphosphorylated tau and disease-related conformational tau epitopes was tested. The monoclonal antibody CP13 recognizes phosphorylated tau serine 202. CP13 labeled diffuse or finely granular perikaryal cytoplasmic neuronal immunoreactivity from 1 month to 8 months (Figure 2e). The distribution of CP13-immunoreactivity was similar to that found with the human-specific antibody T-14, demonstrating that the human tau was hyperphosphorylated within the earliest interval tested, 3 weeks. Antibodies to other pathological epitopes described in NFTs confirmed similar neuronal pathology in rats to that seen in human disease. The monoclonal tau antibody AT100, which specifically recognizes relatively AD-specific phosphorylated serine residues (Ser212 and Ser214), showed a different pattern than CP13, appearing mainly in varicose neurites near the injection sites rather than in neuronal cell bodies. Staining with AT100 was less widespread than with CP13. The Alz-50 antibody, which recognizes an abnormal tau conformation found in AD, gave similar results as AT100 with the pCB-Tau AAV vector. With the pTau-W AAV vector, the neurofibrillary pathology reflected by Alz-50 staining (Figure 3a) appeared more intense and over larger tissue volumes than after comparable injections of pCB-Tau AAV (not shown). It appeared that a larger fraction of the total human tau T-14 immunoreactivity was also positive for Alz-50 in the case of the WPRE vector. The pTau-W vector expressed immunoreactivity for the NFT-related conformational epitope Ab-39 in cell bodies and processes throughout the medial septum (Figure 3b). Gallyas silver staining, which labels fibrillary argyrophilic lesions, revealed NFTs and neuritic processes 3 weeks after injection of the pCB-Tau AAV (Figure 3c). Argyrophilia was examined on sections adjacent to those used for CP13 immunolabeling (Figure 3, d and e). Only some of the CP13-immunoreactive cells, ie, those with globose immunoreactivity, demonstrated silver staining.

Samples processed for transmission electron microscopy (EM) showed neuronal cell bodies and cell processes containing 15- to 20-nm diameter straight filaments (not shown), consistent with P301L tau filaments detected in NFTs in transgenic mice.[12,14] Immunoelectron microscopy demonstrated unequivocally that these filamentous lesions contained tau. Immunoelectron microscopy with CP13 showed immunolabeling of 15- to 20-nm diameter straight filaments (Figure 3f). Similar ultrastructural results were also obtained with a polyclonal antibody specific to human tau (E-1) and with a monoclonal antibody (MC-1) specific to a pathological conformation found in tau in AD. Tau immunoreactivity was detected at the electron microscopic level at 2 months, but the number of gold particles was sparse. There were no pathological filaments or identifiable NFTs at 2

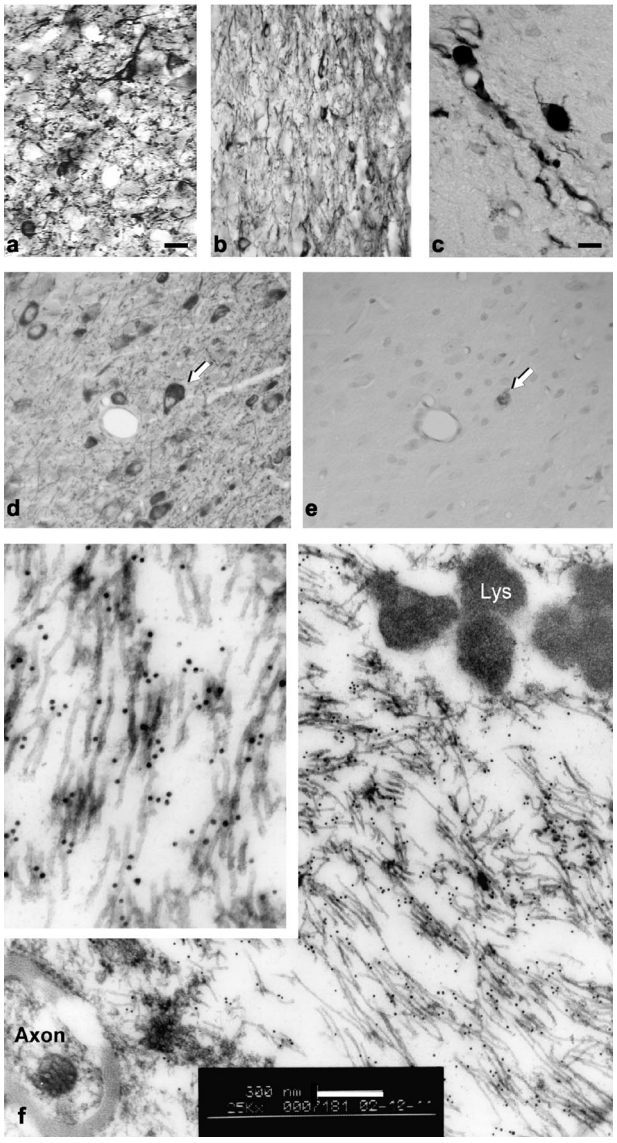

Figure 3. Neurofibrillary pathology and NFT formation in the rat brain. **a:** Alz-50 staining after injection of the WPRE-containing Tau vector, 1×10^{10} particles, 1 month after injection. The Alz-50 staining was more pronounced than with the pCB-Tau AAV (not shown), although this conformational epitope was still mainly expressed in fine neurites. **b:** The NFT-specific antibody Ab-39 labeled dystrophic cells and neurites along the needle track at 4 months, pTau-W AAV. **c:** Gallyas silver staining was detected in neuron cell bodies and processes at 3 weeks after injection, pCB-Tau AAV, 1×10^{10} particles. **d** and **e:** Labeling on adjacent sections with CP13 and Gallyas staining showed that a small fraction of CP13-positive cells were argyrophilic. The globose staining for CP13 (**arrow** in **d**) was also positive for Gallyas (**arrow** in **e**), confirmed NFT at 4 months, pTau-W AAV. **f:** Immunoelectron microscopy was performed using the CP13 antibody. At 4 months, gold particles labeled along 15- to 20-nm filaments, which were found aggregated into bundles, pTau-W AAV. **Inset**, threefold higher magnification. Lys, lysozome. Similar results were found with the conformational MC-1 antibody and the human-specific E-1 antibody. Scale bars: 20 μm (**a**, **b**, **d**, **e**); 8 μm (**c**); 300 nm (**f**).

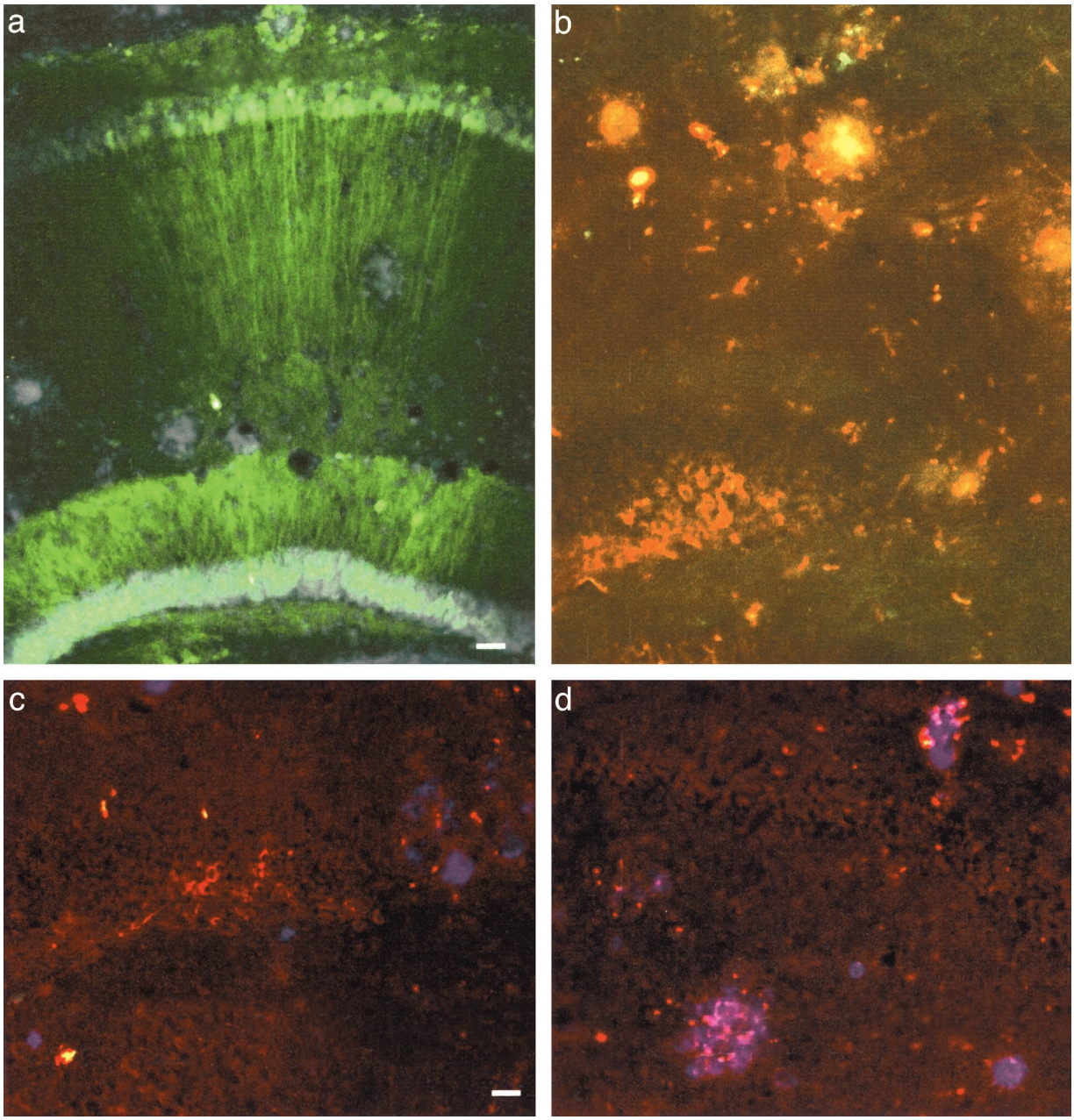

Figure 4. GFP and tau expression in amyloid-bearing mice. **a:** The GFP control vector, pTR-UF12[15,19] was efficient for expression in CA1 and dentate gyrus granule cells after hippocampal injections to PS1/APP double-transgenic mice, 6×10^9 particles in 2 μl injected, 12 months after injection, DAPI counterstain, midline to right. The DAPI-dense loci proved to be amyloid plaques on adjacent sections stained with the 6E10 antibody. **b:** Tau T-14 immunofluorescence (red) in cell bodies and processes in the dentate gyrus, midline to left, 6×10^9 particles of pCB-Tau AAV injected, 12 months after injection. The T-14-stained neurites appeared to be enriched around loci the size of plaques. The green fibers are commissural axons of neurons transduced by GFP control vector injected on the contralateral side as in **a**. **c:** Anti-NFT antibody staining (red) and 6E10 staining (blue) after injections as in **b**. **d:** Plaques near the pCB-Tau AAV injections were surrounded by rings of anti-NFT staining as in **c**. Scale bars: 60 μm (**a**, **b**); 30 μm (**c**, **d**).

months. Some neurons also showed pretangle-like staining patterns at 4 months as was found at earlier intervals.

We injected vectors into the hippocampi of 2-month-old doubly transgenic PS1/APP mice, attempting to add neurofibrillary pathology to an existing transgenic line relevant to AD. The GFP control vector produced efficient transfection of pyramidal and nonpyramidal neurons in CA1 and dentate gyrus that lasted at least 12 months (Figure 4a). After delivery of pCB-Tau AAV, similarly persistent expression in ipsilateral dentate granule neurons was demonstrated by immunoreactivity for the human-specific tau T-14 antibody (Figure 4b). Immunolabeling with a panel of tau antibodies revealed that the pCB-Tau AAV vector produced neuronal tau pathology in the mouse hippocampus similar to that observed with injections into the septal region of rats. Both thioflavine S fluorescence and immunofluorescence for amyloid, demonstrated with a monoclonal antibody to an amino-terminal epitope in Aβ (6E10), showed amyloid deposits throughout the hippocampus and cortex. Some neurons

with tau-immunoreactive pretangles were found in close proximity to amyloid deposits (Figure 4c). The amyloid plaques were also frequently penetrated and surrounded by tau-immunoreactive neurites (Figure 4d), reminiscent of neuritic dystrophy associated with plaques in AD.[25]

Discussion

Human mutant P301L tau was expressed in the brains of adult rats and mice with somatic cell gene transfer. The rat is a versatile animal model for many pharmacological and behavioral probes. The expression of NFTs, perhaps the most common neuropathological lesions found across the broadest range of neurodegenerative diseases, in this species will facilitate studies of factors that influence NFT formation. For example, the influence of the aged brain can be evaluated by comparing results from vector injections at the same dose and time interval, in either young or old rats. Such an experiment would be difficult in existing models of tauopathy, but addressable with a vector approach because the onset of transgenic expression can be controlled. Another advantage of this approach is the ability to combine transgenes, which we demonstrated by expressing at least pretangle tau pathology in the brains of amyloid mice. We found tau-immunoreactive neurites closely associated with amyloid plaques. This approach may therefore provide a novel experimental method to model AD pathology comprehensively, in which relationships between amyloid and tau *in vivo* can be analyzed systematically.

The degree of tau pathology appeared to be expression level- and time-dependent. The combination of the CBA promoter and the WPRE in AAV serotype 2 vectors boosted expression levels of tau in neurons to significantly higher levels than in similar vectors without the WPRE, with the CBA-tau-WPRE AAV producing detectable tau expression in primary neuronal cultures, whereas the CBA-tau AAV did not. The greater expression of tau conferred by the WPRE also led to greater pathology because a more complete fraction of the total tau immunoreactivity was also positive for Alz-50 immunoreactivity in the case of the CBA-tau-WPRE vector. Expressing more tau within neurons apparently led to more AD-like Alz50 tau conformations. NFTs were unequivocally detected by immunoelectron microscopy at 4 months but not at 2 months, suggesting that NFT formation was time-dependent throughout this interval in this model. The sparse pretangle-like deposition of gold particles observed at 2 months was also found in some neurons at 4 months, which may suggest that NFT formation is not complete by 4 months. The fact that positive Gallyas staining could be found in a few cells within 3 weeks suggests that NFT formation may be occurring much faster in some cells, perhaps those expressing the highest levels of tau or specific cell types that are more tangle-genic, potentially because of differential expression of kinases that may phosphorylate tau.

The vector approach can be used to successfully model NFTs in adult rats. This model will be useful for studying the pathogenesis of neurodegeneration. The ability to target specific neuronal populations affected in human disease makes it possible to generate animal models that are more complete approximations of specific diseases, which may facilitate the development of rational therapeutic interventions.

Acknowledgments

We thank Dr. P. Davies (Albert Einstein College of Medicine, Bronx, NY) for antibodies CP13, Alz-50, and MC-1; Dr. S. H. Yen (Mayo Clinic, Jacksonville, FL) for antibodies E-1 and Ab-39; and Craig Meyers and Aaron Hirko for technical contributions.

References

1. Hutton M, Lendon CL, Rizzu P, Baker M, Froelich S, Houlden H, Pickering-Brown S, Chakraverty S, Isaacs A, Grover A, Hackett J, Adamson J, Lincoln S, Dickson D, Davies P, Petersen RC, Stevens M, de Graaff E, Wauters E, van Baren J, Hillebrand M, Joosse M, Kwon JM, Nowotny P, Che LK, Norton J, Morris JC, Reed LA, Trojanowski J, Basun H, Lannfelt L, Neystat M, Fahn S, Dark F, Tannenberg T, Dodd PR, Hayward N, Kwok JBJ, Schofield PR, Andreadis A, Snowden J, Craufurd D, Neary D, Owen F, Oostra BA, Hardy J, Goate A, Swieten JV, Mann D, Lynch T, Heutink P: Association of missense and 5′-splice-site mutations in tau with the inherited dementia FTDP-17. Nature 1998, 393:702–705
2. Spillantini MG, Bird TD, Ghetti B: Frontotemporal dementia and parkinsonism linked to chromosome 17: a new group of tauopathies. Brain Pathol 1998, 8:387–402
3. Binder LI, Frankfurter A, Rebhun LI: The distribution of tau in the mammalian central nervous system. J Cell Biol 1984, 101:1371–1378
4. Stamer K, Vogel R, Thies E, Mandelkow E, Mandelkow EM: Tau blocks traffic of organelles, neurofilaments, and APP vesicles in neurons and enhances oxidative stress. J Cell Biol 2002, 156:1051–1063
5. Bancher C, Brunner C, Lassmann H, Budka H, Jellinger K, Wiche G, Seitelberger F, Grundke-Iqbal I, Iqbal K, Wisniewski HM: Accumulation of abnormally phosphorylated tau precedes the formation of neurofibrillary tangles in Alzheimer's disease. Brain Res 1989, 477: 90–99
6. Buee L, Bussiere T, Buee-Scherrer V, Delacourte A: Tau protein isoforms, phosphorylation and role in neurodegenerative disorders. Brain Res Brain Res Rev 2000, 33:95–130
7. van Slegtenhorst M, Lewis J, Hutton M: The molecular genetics of the tauopathies. Exp Gerontol 2000, 35:461–471
8. Braak E, Braak H, Mandelkow EM: A sequence of cytoskeleton changes related to the formation of neurofibrillary tangles and neuropil threads. Acta Neuropathol (Berl) 1994, 87:554–567
9. Weaver CL, Espinoza M, Kress Y, Davies P: Conformational change as one of the earliest alterations of tau in Alzheimer's disease. Neurobiol Aging 2000, 21:719–727
10. Alonso AC, Grundke-Iqbal I, Iqbal K: Alzheimer's disease hyperphosphorylated tau sequesters normal tau into tangles of filaments and disassembles microtubules. Nat Med 1996, 2:783–787
11. Kowall NW, Kosik KS: Axonal disruption and aberrant localization of tau protein characterize the neuropil pathology of Alzheimer's disease. Ann Neurol 1987, 22:639–643
12. Lewis J, McGowan E, Rockwood J, Melrose H, Nacharaju P, Van Slegtenhorst M, Gwinn-Hardy K, Paul Murphy M, Baker M, Yu X, Duff K, Hardy J, Corral A, Lin WL, Yen SH, Dickson DW, Davies P, Hutton M: Neurofibrillary tangles, amyotrophy and progressive motor disturbance in mice expressing mutant (P301L) tau protein. Nat Genet 2000, 25:402–405
13. Götz J, Chen F, Barmettler R, Nitsch RM: Tau filament formation in transgenic mice expression P301L tau. J Biol Chem 2001, 5:529–534
14. Lin WL, Lewis J, Yen SH, Hutton M, Dickson DW: Filamentous tau in oligodendrocytes and astrocytes of transgenic mice expressing the human tau isoform with the P301L mutation. Am J Pathol 2003, 162:213–218

15. Klein RL, King MA, Hamby ME, Meyer EM: Dopaminergic cell loss induced by human A30P alpha-synuclein gene transfer to the rat substantia nigra. Hum Gene Ther 2002, 13:605–612
16. Holcomb L, Gordon MN, McGowan E, Yu X, Benkovic S, Jantzen P, Wright K, Saad I, Mueller R, Morgan D, Sanders S, Zehr C, O'Campo K, Hardy J, Prada CM, Eckman C, Younkin S, Hsiao K, Duff K: Accelerated Alzheimer-type phenotype in transgenic mice carrying both mutant amyloid precursor protein and presenilin 1 transgenes. Nat Med 1998, 4:97–100
17. Niwa H, Yamamura K, Miyazaki J: Efficient selection for high-expression transfectants with a novel eukaryotic vector. Gene 1991, 108: 193–199
18. Loeb JE, Cordier WS, Harris ME, Weitzman MD, Hope TJ: Enhanced expression of transgenes from adeno-associated virus vectors with the woodchuck hepatitis virus posttranscriptional regulatory element: implications for gene therapy. Hum Gene Ther 1999, 10:2295–2305
19. Klein RL, Hamby ME, Gong Y, Hirko AC, Wang S, Hughes JA, King MA, Meyer EM: Dose and promoter effects of adeno-associated viral vector for GFP expression in the rat brain. Exp Neurol 2002, 176: 66–74
20. Chou YC, Luttge WG, Sumners C: Characterization of glucocorticoid type II receptors in neuronal and glial cultures from rat brain. J Neuroendocrinol 1990, 2:29–38
21. Zolotukhin S, Byrne BJ, Mason E, Zolotukhin I, Potter M, Chesnut K, Summerford C, Samulski RJ, Muzyczka N: Recombinant adeno-associated virus purification using novel methods improves infectious titer and yield. Gene Therapy 1999, 6:973–985
22. Grimm D, Kern A, Rittner K, Kleinschmidt JA: Novel tools for production and purification of recombinant adeno-associated virus vectors. Hum Gene Ther 1998, 9:2745–2760
23. Paxinos G, Watson C: The Rat Brain in Stereotaxic Coordinates. San Diego, Academic Press, 1998
24. Paxinos G, Franklin KBJ: The Mouse Brain in Stereotaxic Coordinates. San Diego, Academic Press, 2001
25. Dickson DW: The pathogenesis of senile plaques. J Neuropathol Exp Neurol 1997, 56:321–339